CALCIUM DIFFUSION IN TRANSIENT AND STEADY STATES IN MUSCLE

ROBERT E. SAFFORD, *Department of Physiology and Biophysics, Mayo Graduate School of Medicine and Mayo Medical School, Rochester, Minnesota 55901*
AND
JAMES B. BASSINGTHWAIGHTE, *Center for Bioengineering, University of Washington, Seattle, Washington 98195 U.S.A.*

ABSTRACT Rates of diffusion through the extracellular space of thin sheets of myocardium from the right ventricular outflow tract of kittens were estimated at 23°C for $^{45}Ca^{2+}$ and an inert reference tracer, [^{14}C]sucrose. The myocardial sheets were mounted in an Ussing chamber and equilibrated with Tyrode solution with varied calcium concentrations, Ca_0. The tracers were added to one side and their concentrations on the other side measured at 5–15-min intervals for 6 h. The apparent tracer diffusion coefficient for sucrose was $1.11 \pm 0.06 \times 10^{-6}$ cm^2s^{-1} (mean ± SEM, $n = 74$), 22% of the free diffusion coefficient; the lag time before reaching a steady state provided estimates of the intratissue volume of distribution or diffusion space of 0.41 ± 0.15 ml/ml tissue ($n = 74$), a value compatible with expectations for extracellular fluid space. Over the range of Ca_0 from 0.02 to 9.0 mM, the intratissue apparent diffusion coefficient for Ca, D_{Ca}, averaged $1.65 \pm 0.10 \times 10^{-6}cm^2s^{-1}$, $n = 74$, which is 21% of the free D^0_{Ca}, and was not influenced by Ca_0. Because transsarcolemmal Ca permeation is slow, D_{Ca} is the diffusion coefficient in the extracellular region. The paired ratios D_{Ca}/D_s averaged 1.32 ± 0.05 ($n = 67$) for all levels of Ca_0 but at physiologic or higher Ca_0 averaged 1.45 ± 0.07 ($n = 39$), close to the ratio of free diffusion coefficients, 1.53. Equations distinguishing transient from steady state diffusion were fitted to the data, showing that the apparent distribution volume of "binding sites" external to the diffusion pathway diminished at higher Ca_0 in a fashion suggesting that at least two different Ca^{2+} binding sites were present.

INTRODUCTION

A thorough understanding of the diffusional processes involved in blood-tissue exchange of substrates and metabolites is critical to the interpretation of observations of gradients and fluxes made after changes in the concentration of a substance at a point in a system. Studies of kinetics often utilize tracers, and it is therefore important to define the restricted circumstances under which the movement of an isotopic marker represents the movement of the unlabeled mother substance. The kinetics of transient movement of a tracer ion at a time when the mother substance, the

---

Dr. Safford's present address is: Department of Internal Medicine, Massachusetts General Hospital, Boston, Mass. 62114.
Address reprint requests to Dr. Bassingthwaighte.

traced ion, is in steady state describe the steady state kinetics, but may not describe a transient process for the traced ion, for example for diffusion in the presence of binding sites for the ion.

The diffusional movement of calcium through the extracellular space (ECS) of muscle is of particular interest since Ca^{2+} is a key factor in excitation-contraction coupling and in other regulatory processes at cell surfaces. Binding to mobile and immobile sites will affect Ca^{2+} movement. The extracellular space contains ground substances with a net negative charge at physiological pH (mucopolysaccharides, or glycosaminoglycans, chondroitin sulfate B, and hyaluronic acid) which affect the distribution of cations in extracellular fluid (ECF) (Gersh and Catchpole, 1960, Engel et al., 1961; Haljamäe et al., 1974) and bind calcium avidly (Aldrich, 1958; Manery, 1966). Cation binding sites also appear to be present in the basement membrane of the T system, where deposits of La^{3+} have been seen in electron micrographs (Philpott and Goldstein, 1967; Martinez-Palomo et al., 1973). Possible binding sites on the sarcolemma include the carrier for coupled Na-Ca exchange (Reuter and Seitz, 1968) or K-Ca exchange (Morad and Goldman, 1973), the channels for the slow inward current (Beeler and Reuter, 1970), and the materials of the basement membrane (Langer and Frank, 1972). These binding substances probably serve also as ion exchangers since other ions can be expected to compete for the sites that attract Ca^{2+}. Thus, the electrochemical environment of a calcium ion in cardiac muscle may well be influenced by at least three physiological classes of extracellular binding sites: negative charges within the ground substances that presumably might "buffer" changes in Ca_0 (calcium concentration in the ECF), sites on the sarcolemma, and sites on albumin and other soluble proteins in the ECF. Of these three, the ground substances are probably the most important quantitatively. In addition, cellular uptake may contribute to the sequestration, but this will be small since the total cell calcium content is low. The experimental method we present here is directed toward estimating the diffusion coefficients and cannot provide refined information on binding kinetics.

The diffusion of Ca^{2+} ion in muscle has been considered rather slow compared to that expected from the free diffusion coefficient in water, D^0_{Ca}. Niedergerke (1957) estimated the apparent diffusion coefficient for the extracellular diffusion of Ca in frog heart to be one sixteenth of D^0_{Ca}, estimating tissue ECF Ca^{2+} concentrations from the rates of change of tension developed with each beat after a change in perfusate Ca_0.

Kushmerick and Podolsky (1969) estimated the diffusion coefficient of Ca^{2+} in the sarcoplasmic fluid of skinned frog skeletal muscle fibers to be one fiftieth of D^0_{Ca}; binding of Ca^{2+} to sarcoplasmic reticulum and contractile protein was recognized as contributing to the slowing of the diffusional process.

We will argue that these values are too low to represent steady state diffusion coefficients; our view is not greatly different from Niedergerke's but emphasizes a need for a particular clarification: the diffusion coefficient is a measure of the rate of movement of the species through a specific milieu; the binding capacity of the milieu is an independent parameter. Under rather specific circumstances, the rate of movement of a wave of concentration can be described by an apparent diffusion coefficient, D'_{Ca},

resulting from the combination of diffusion and capacitative buffering due to binding:

$$D'_{Ca} = D^0_{Ca}/\lambda^2 \cdot V_{diff}/(V_{diff} + V_{bind}), \quad (1)$$

where λ is the tortuosity factor, V_{diff} is the volume of the diffusion channel, and V_{bind} is the volume of distribution of the bound calcium. (V_{bind} is a virtual volume in which the apparent concentration is the same as in the diffusion channel.) V_{bind} includes all sites with which Ca^{2+} exchanges, but which do not contribute to the diffusional movement: side channels or dead-end pores (Goodknight and Fatt, 1961) or binding to immobile sites. Components of V_{bind} may in theory be distinguished if they have differing binding constants or react at rates slower than the diffusional rates. In our experiments the diffusional time lag is probably very long compared to time required for binding, so in our mathematical approach we will consider the several possible components of V_{bind} to be indistinguishable and will lump them together. We will also neglect the contribution of mobile Ca^{2+} binding sites to the diffusion, for what little information we have suggests that albumin-bound Ca^{2+} and other such complexes are in low concentration and diffuse slowly.

The presence of immobile binding sites along a diffusion pathway will retard a wave of increasing concentration. The retardation is essentially a capacitance phenomenon; the buffering of changes in Ca^{2+} concentration and the retardation are proportional to the number of binding sites. For tracer, the duration of a transient state depends on the number of binding sites occupied by unlabeled mother substance, V_{bind}. Thus, at concentrations of mother substance (unlabeled Ca^{2+}) that are high relative to the dissociation constant for binding, most of the sites will be occupied by mother substance and the volume of distribution for the tracer will be relatively large and the retardation great. On the other hand, when the concentration of mother substance is so low that most of the binding sites are unoccupied, even though a relatively high fraction of both the traced and tracer Ca^{2+} are bound to the immobile sites, the apparent volume of distribution and the duration of the transient will be small.

The tortuosity coefficient, λ, is the ratio of the path length taken by molecules traversing the region available for diffusion, the "diffusion channel," to the macroscopic minimum path length of the channel, i.e. the tissue thickness. One may reasonably expect similar tortuosities for a large class of solutes for which the impediments to diffusion are similar; for example, for diffusion across a field of parallel cylinders a tortuosity, λ, of 2 is expected for all molecules that are small compared with the cylinder diameters (Johnson and Stewart, 1965). See Appendix I, which shows why λ is squared.

V_{diff}, the volume of the diffusional channel, may be expected to be nearly constant for a variety of small hydrophilic solute species. As molecular size increases, however, molecular exclusion from increasing fractions of the water in the diffusion channel can decrease V_{diff} if the diffusion is occurring through a gel matrix (or a sol-gel combination) whose interstices are not greatly larger than the solute molecules (see, for example, Fig. 6 of Laurent, 1970). Collagen, chondroitins, and hyaluronates provide

the basis for this matrix in myocardium; albumin and other large mobile and immobile molecules will contribute further to any exclusion phenomena (Shaw, 1976).

Now, to our key argument: Eq. 1 should apply whenever a solute species is undergoing a change in concentration. If there were a step increase in concentration of free unlabeled calcium, Ca_0, then $D'_{Ca}/(D^0_{Ca}/\lambda^2)$ or $V_{diff}/(V_{diff} + V_{bind})$ is the speed of the front of increasing concentration relative to the speed in the absence of binding, and V_{bind} is the increment in the volume of distribution of Ca^{2+} induced by the increase in Ca_0. The complementary argument holds for a decrease in Ca_0. For a step increase in tracer concentration from zero, V_{bind} is the whole of the exchangeable Ca^{2+} neighboring the diffusion channel; Eq. 1 will be apropos when the diffusion front itself can be observed, as in the experiments of Hodgkin and Keynes (1953), Weidmann (1966), Kushmerick and Podolsky (1969), Caillé and Hinke (1972), and Weingart (1974).

But Eq. 1 is not appropriate for steady-state experiments, such as those of Page and Bernstein (1964), and Suenson et al. (1974). In the steady state, the flux of tracer across a sheet of muscle is unaffected by binding since the intratissue specific activity remains constant, and:

$$D_{Ca} = D^0_{Ca}/\lambda^2, \tag{2}$$

where D_{Ca} is an effective or apparent intratissue diffusion coefficient. The simplicity results from the constancy of V_{bind}, so that there is no loss of tracer $^{45}Ca^{2+}$ from the diffusion channel to the binding sites. Thus Page's (1963) value for D_{Ca} of $\frac{1}{4}$ of D^0_{Ca} for a steady-state experiment in cat heart is the value expected from the values of $\lambda^2 = 4$ found later by Suenson et al. (1974) for sucrose and sodium in the same experimental preparation.

Mammalian cardiac muscle is a good model on which to test diffusional phenomena since it has a well characterized, fairly regular structure, as can be seen in the studies of Fawcett and McNutt (1969) and Polimeni (1974). The technique of Page and Bernstein (1964) and Suenson et al. (1974), using thin, regular sheets of muscle from the right ventricular outflow tract of young cats and kittens, is particularly valuable because the muscle can be kept viable for hours in an artificial medium, and without any convective flow (of blood or perfusate) to complicate the analysis. Patlak and Fenstermacher (1975) did study diffusional transport into intact blood-perfused brain, looking at tracer concentration profiles as a function of distance from the floor of the fourth cerebral ventricle, and obtained estimates of D and capillary permeability based on the absence of binding. While such an approach might be possible in the heart, we felt that since binding processes were involved in our experiments, we had to simplify the approach.

Although in vitro estimates of diffusion coefficients in physical systems tend to be quite accurate (Longsworth, 1953; Stokes, 1950)[1] the accuracy of in vivo estimates leaves much to be desired. For cardiac muscle, Page and Bernstein (1964) found

[1]Gosselin, R. E. 1976. Personal communication.

values of D'/D^0 of about $\frac{1}{2}$ for sucrose, while Suenson et al. (1974) obtained lower estimates, about $\frac{1}{4}$. The difference has not been explained; we will present evidence in support of D'/D^0 being $\frac{1}{4}$ for sucrose, water, and Ca^{2+}. Clear evidence of exclusion phenomena or restricted diffusion is lacking but might be provided by experiments on larger molecules.

METHODS

We excised the upper anterior free wall of the right ventricle of 42 cats ranging in weight from 0.6 to 1.5 kg. Although the myocardium of kittens may not be completely mature, it was important that the preparations be thin enough to be well oxygenated, as discussed by Suenson et al. (1974). The 1–2-mm-thick sheet of myocardium with endothelium on both sides was mounted between the chambers of an Ussing-type diffusion cell so that a relatively smooth circular sheet 0.6 cm in diameter (total area A_T = 0.283 cm^2) was exposed to the same Krebs-Ringer solution on both surfaces, as described in more detail previously (Suenson et al., 1974). The standard solution contained (mM): Na 145, K 5.4, Ca 1.8, Mg 0.5, Cl 133, HCO_3 24, H_2PO_4 0.4, glucose 2.2; the measured pH's ranged from 7.35 to 7.45 after equilibration with 95% O_2, 5% CO_2 gas. Ca_0 was varied from 0.21 to 9.2 mM without significantly changing the concentrations of the other solutes. In 13 experiments Na_0 was reduced to 24 mM by sucrose substitution to maintain osmolality at approximately 300 mosmol. To minimize the unstirred layer at the solution-tissue interface, each chamber of the cell was agitated by a magnetic stirring bar, and streams of bubbles of 95% O_2–5% CO_2 were directed upwards across both surfaces of the disk of muscle.

After $1\frac{1}{2}$–2 h (a time roughly equal to the duration of the diffusional transient) for equilibration between the tissue and the bathing media, $^{45}CaCl_2$ and [^{3}H]- or [^{14}C]-sucrose were added at high specific activity (100 μCi) to the 14-ml chamber facing the epicardial surface of the muscle sheet ("donor" chamber with concentration, C_D^*). After addition of tracer, samples (200 μl) were taken from the "recipient" chamber facing the endocardial surface providing the tracer concentration $C_R^*(t)$ at regular intervals (2–15 min) of time, t, for 6 h or more. Each sample from the recipient chamber was replaced with an equal volume of unlabeled solution to maintain the equality of hydrostatic pressures in each chamber. These samples were counted in a Nuclear-Chicago Mark II 3-channel liquid scintillation counter (Nuclear-Chicago Corp., Des Plaines, Ill.) with windows set to discriminate between ^{45}Ca, ^{14}C, and ^{3}H, and, by using an inbuilt automatically counted external standard, the observed sample count rates were corrected for background, isotope spillovers, variations in counting efficiency and for the amount of tracer removed with each sample to provide estimates of $C_R^*(t)$. C_D^* was considered constant. (Samples taken in duplicate from the donor chamber at the start and at the end of the experiment differed by only 0.2–1%, justifying assuming constancy.) The relative concentration in the unlabeled recipient chamber was $C_R(t)$, calculated as $C_R(t) = C_R^*(t)/C_D^*$.

Experiments were done at room temperature, 22–24°C. At this temperature, O_2 consumption is relatively low; it seemed assured that the oxygen supply to this preparation was adequate at 37°C (Suenson et al., 1974), but at the lower temperature one's confidence in the calculation is greater. Additional tests guaranteeing viability of each preparation were done on occasional preparations: the resting membrane potentials at the end of 2 h of equilibration and 6 h of experimentation without glucose were −39 to −45 mV; this implies that the myocardial cells were somewhat depolarized but that the sarcolemma was still quite impermeable to ions. In one series the water content of the tissue was measured at the end, and found to be 0.783 ± 0.0088 g/g wet weight, n = 30 (mean ± SD,); this is close to the 0.796 ± 0.040 (n = 10) found by Suenson et al. (1974) and the 0.774 ± 0.046 found by Page and Bernstein (1964) in cat hearts and does not indicate more swelling than normal.

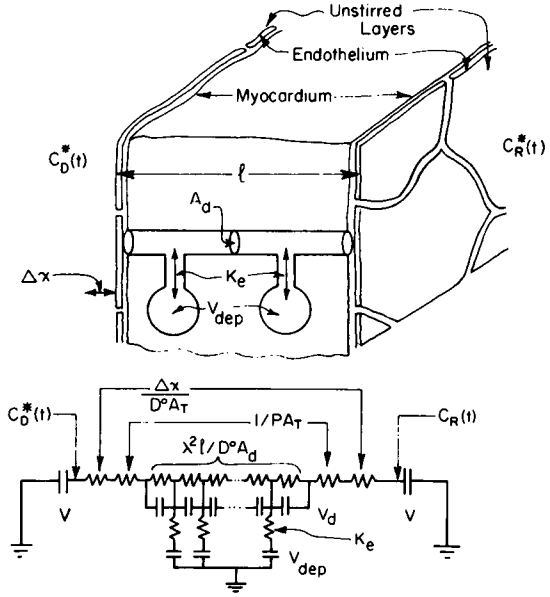

FIGURE 1

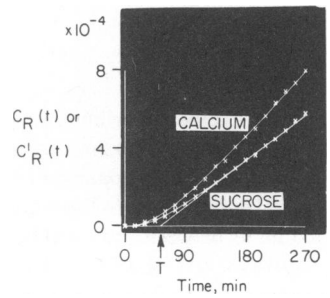

FIGURE 2

FIGURE 1 Diagram of sheet of myocardium across which diffusion occurs. The presence of endothelium and of unstirred layers adds resistances in series. The circuit diagram below is an approximation providing a conceptual basis for the equation describing the diffusional processes. (V_d is the sum of the capacitances in series, V_{dep} is the sum of those in parallel.) All resistances are in seconds per cubic centimeter: $\Delta x/D^0A_T$ for an unstirred layer, $1/PA_T$ for endothelium.

FIGURE 2 Relative concentration versus time curves [$C_R(t)$] for calcium and sucrose. X's are experimental data points. A straight line of slope 2.8×10^{-4} min^{-1} has been drawn through the steady state portion of the sucrose curve yielding a "time-lag", T, of 58 min. $C'_R(t)$, computed from Eq. 3, the model for the homogeneous sheet of uneven thickness ($n = 9$ pathways, $\bar{l} = 0.120$ cm) is the curved line fitting the entire curve, yielding $D_s = 0.71 \times 10^{-6}$ cm^{2}s^{-1} and $A_d/A_T = 0.39$. The model for the uneven sheet with dead-end pore volumes, Eq. 10, has been fitted to the calcium curve yielding $D_{Ca} = 1.75 \times 10^{-6}$ cm^{2}s^{-1}, $V_{dep}V_d = 1.65$, and $K_e = 2.5 \times 10^{-3}$s^{-1}. (See text for discussion of model.)

ANALYTICAL METHODS

The analysis provides two main approaches to solute diffusion across an uneven but nearly planar slab; the first is suited to solutes such as sucrose that are not bound or otherwise sequestered within the slab; the second provides for solute binding or sequestration within regions aside from the diffusion path, i.e. dead-end pores, an analysis suited to the diffusion of calcium. The general concepts are diagrammed in Fig. 1; the essential concept is that the myocardium comprises a distributed resistance and capacitance for each pathway. The presence of binding simply enlarges the capacitance without reducing the resistance. Some further analysis is provided to account for details of the experimental situation, accounting for or estimating the effects of boundary layers (unstirred layer effects and penetration of the endothelial lining), of bidirectional fluxes of tracer ("back diffusion" of tracer), loss from the donor chamber, and of solute partitioning between the bathing media and the diffusion channel.

Parallel Pathway Analysis for a Homogeneous but Uneven Sheet

This is an extension of the equation for diffusion across a uniform plane sheet (Barrer, 1953) to account for variation in thickness or diffusion path length, as described by Suenson et al. (1974). The disk is considered to consist of N independent parallel pathways of relative cross-sectional area w_i and length l_i. To determine w_i and l_i the tissue was cut into five or six parallel strips taken near the diameter of the disk, and the thickness from epicardium to endocardium measured at 0.2-mm intervals to provide a frequency distribution of the fractional areas of the disk, w_i, having diffusion paths of lengths, l_i, perpendicular to the plane of the disk, and a mean thickness, $\bar{l}$, which is $\sum_{i=1}^{N} w_i l_i$. The weighting function has unity area: $\sum_{i=1}^{N} w_i = 1.0$. The mean thicknesses of the disks were 0.86–2.24 mm. and their relative dispersions (SD's of the l's divided by the mean, $\bar{l}$) were 3.9–28.0%.

Plots of $C_R(t)$, illustrated for calcium and sucrose in Fig. 2, were curved during the early part of an experiment but became linear as the steady-state tracer concentration gradient within the disk was attained. The duration of an experiment was long enough that the apparently linear steady state (determined visually) existed for at least 90 min for the more slowly diffusing tracer. (Extrapolation of this linear portion of a curve gives the abscissal intercept or "time-lag," T.) Applying the equation for diffusion across a plane (Crank, 1956) to each pathway and summing their responses provide a composite theoretical curve, $C'_R(t)$, comparable to the experimental curve, $C_R(t)$;

$$C'_R(t) = \frac{DA_d t}{V} \sum_{i=1}^{i=N} \frac{w_i}{l_i} - \frac{\bar{l} A_d}{6V} + \sum_{i=1}^{i=N} \frac{2 w_i l_i A_d}{\pi^2 V} \sum_{m=1}^{m=M} \frac{(-1)^m}{m^2} \cdot (\exp(-Dm^2\pi^2 t/l_i^2)), \quad (3)$$

where D is the diffusion coefficient (cm^2/s) in the tissue, A_d is the area (cm^2) through which diffusion occurs, t is time (s), V is the volume of the recipient chamber (14 ml), and M is the number of terms in the summation of the series (20 sufficed) in the transient part of the solution on the second line. Eq. 3 was used for sucrose: first, D_s, the diffusion coefficient for sucrose and A_d, its diffusional area, were determined from the first term on the right giving the steady state slope (from the 3rd or 4th to the 6th hour), dC_R/dt, and the time-lag T_s, which is the intercept given by the first and second terms at $t = T_s$ when $C'_R(t) = 0$. By the forms shown previously by Suenson et al. (1974):

$$D_s = \frac{\bar{l}}{6T \sum_{i=1}^{i=N} (w_i/l_i)} \quad (4)$$

$$A_d = (V/[D_s \Sigma(w_i/l_i)]) \cdot [dC_R(t)/dt] = (6T_s/\bar{l}) \cdot (V dC_R(t)/dt). \quad (5)$$

To check the applicability of this model for each experiment, the theoretical curve, $C'_R(t)$, was computed from D_s and A_d from Eqs. 4 and 5 and was observed to fit not only the linear portion but also the transient (curved) portion of the experimental $C_R(t)$, as shown in Fig. 2. The diffusional area for calcium was assumed to equal that for sucrose, A_d. The volume of the diffusion channel, V_d, is taken to be the same for sucrose and calcium, is conceptually identical to V_{diff}, and is defined by:

$$V_d = A_d \bar{l}. \quad (6)$$

The volume of distribution of sucrose, as a fraction of the tissue volume is simply $V_d/A_T\bar{l}$ or A_d/A_T, ml/ml tissue, where A_T is the total area of one surface of the tissue slab.

Parallel Pathway, Dead-End Pore Model Accounting for Sequestration or Binding

The curves for calcium could not be fitted by a planar diffusion model including either a single or multiple independent pathway, but required an additional feature, sequestration of calcium within the tissue, to account for an abscissal intercept that was delayed relative to that for sucrose.

The dead-end pore model of Goodknight and Fatt (1961) includes a volume, V_{dep} (ml/ml tissue), with which tracer in the diffusion channel equilibrates, increasing the transport delay, T, across the disk of tissue. V_{dep} is the sum of all the different binding sites or sequestered spaces. The solution to the diffusion equation for a homogeneous membrane of uniform thickness, $\bar{l}$, containing a uniform distribution of dead-end pores is:

$$C'_R(t) = DA_dt/V\bar{l} - (\bar{l}A_d + V_{dep})/6V + \pi DA_d/V\bar{l}^2 \sum_{m=1}^{M} \frac{m(-1)^m \exp(tS_{+,-})}{S^2_{+,-}\partial\beta/\partial S_{+,-}}. \quad (7)$$

(Eq. 20 of Goodknight and Fatt [1961] contains a typographical error: $S^2_{+,-}$, not $S_{+,-}$ to the first power, should appear in the denominator of their third term.) Here,

$$\beta = m\pi/\bar{l}, \qquad m = 1, 2, \ldots, M, \quad (8a)$$

$$G = K_e(1 + V_{dep}/\bar{l}A_d) + D\beta^2, \quad (8b)$$

$$S_{+,-} = -\frac{G}{2} \pm \frac{1}{2}[G^2 - 4D\beta^2K_e]^{1/2}, \quad (8c)$$

$$\partial\beta/\partial S_{+,-} = \frac{-1}{2D\beta}[1 + (V_{dep}/\bar{l}A_d)K_e/(S_{+,-} + K_e)^2]. \quad (8d)$$

K_e is the rate constant for exchange of tracer between the dead-end pore volume and the diffusion channel volume. Slow equilibration or binding (a low K_e) prolongs the transient phase, retarding the beginning of the steady state portion of $C'_R(t)$. Since $S_{+,-}$ is defined by the roots of a quadratic equation, the summation over the index m in Eq. 7 is really the sum of two series, one for the value of S_+ computed with the plus sign in Eq. 8*c* and a second for S_- computed with the minus sign. Both roots are required for the solution, since neither can be excluded on physical grounds. Five terms ($M = 5$) are sufficient for convergence of the series in the third term of Eq. 7 in most circumstances.

One may apply this single-pathway result to compute $C'_R(t)$ for the situation in which the membrane is considered to consist of N parallel diffusion pathways (each having the same tracer diffusion coefficient D) of length l_i and cross-sectional area available for diffusion w_iA_d (where l_i and w_iA_d substitute for $\bar{l}$ and A_d in Eqs. 7, 8*a*, and 8*b*:

$$C'_R(t) = \sum_{i=1}^{N} (C'_R(t))_i. \quad (9)$$

The result obtained after algebraic simplification is:

$$C'_R(t) = \left[\frac{DA_d t}{V}\sum_{i=1}^{i=N}\frac{w_i}{l_i}\right] - \frac{\bar{l}A_d + V_{dep}}{6V} + \frac{2\pi^2 D^2 A_d^2 \bar{l}}{V}$$

$$\sum_{i=1}^{N}\frac{w_i}{l_i^2}\sum_{m=1}^{5}\left[\frac{m^2(-1)^m \exp(t\cdot S_{+,-})}{S_{+,-}^2(-l_i(A_d\bar{l} + V_{dep}(K_e/(K_e + S_{+,-}))^2))}\right] \quad (10)$$

For Eq. 10, $S_{+,-}$ and its component G must be calculated for each path length with $\beta = m\pi/l_i$ instead of Eq. 8*a*. The mean $\bar{l}$'s in Eqs. 8*c* and *d* are still appropriate. From the steady-state terms, the first two terms in Eq. 10, one can show that the calcium diffusion coefficient and dead-end pore volume are related to the slope, $dC_R(t)/dt$, and time-lag T of the calcium curve, by the following relationships:

$$D = \frac{V}{A_d\sum_{i=1}^{i=N}\frac{w_i}{l_i}}\cdot\frac{dC_R(t)}{dt}. \quad (11)$$

$$V_{dep}/V_d = V_{dep}/\bar{l}A_d = \left[\frac{6DT}{\bar{l}}\sum_{i=1}^{i=N}\frac{w_i}{l_i}\right] - 1. \quad (12)$$

Model Fitting

The first step in the analysis of an experiment was to fit the sucrose data to obtain the time-lag, T_s, and slope, $dC_R(t)/dt$, which were then used to compute D_s and A_d with Eqs. 4 and 5.

Following the same procedure and assuming the diffusional area for calcium to be equal to that for sucrose (which we will justify below by arguing that their partitioning in the diffusion channel must be similar), we computed D_{Ca} and the ratio of dead-end pore volume to diffusion channel volume, V_{dep}/V_d, from the time-lag, T, and the steady state slope of the calcium curve, using Eqs. 11 and 12. The remaining parameter in the dead-end pore analysis, K_e, the rate of exchange between V_d and V_{dep}, has no influence on the steady state slope or time-lag, but determines the curvature of the transient portion of the solution for the dead-end pore model. Using the estimates of D_{Ca}, A_d, and V_{dep}/V_d and the distribution of thicknesses across the muscle disk ($w_i l_i$), complete solutions to the parallel pathway model with dead-end pores were computed from Eq. 10, and K_e was adjusted iteratively until a visual best fit to the transient was obtained.

Additional Factors Modifying the Estimated Diffusion Coefficients

BACK DIFFUSION OF TRACER Maximum values for $C_R(t)$ obtained at t = 6 h did not exceed 0.46% of that in the donor chamber so that, for the purpose of analysis, back diffusion from recipient to donor chamber reduced $C_R(t)$ by a negligible amount, less than 0.2% of $C_R(t)$.

DIFFUSIONAL RESISTANCE OF BOUNDARY LAYERS A barrier composed of two unstirred layers, two permeability barriers, and a slab of tissue is diagrammed in Fig. 1. In the steady state the flux per unit driving force is the reciprocal of the total resistance, which is the sum of the resistances of the three components:

Flux per unit driving force = 1/resistance,

$$V\frac{dC'_R(t)}{dt} = \frac{1}{2\Delta x/(D^0A_T) + 2/(PA_T) + 1/(DA_d\Sigma(w_i/l_i))}. \quad (13)$$

where Δx is the thickness of each unstirred layer of area A_T and in which D^0 is the pertinent, aqueous, diffusion coefficient, P is the permeability of each endothelial surface layer, and the third resistance is that of the tissue slab itself, as in the first term of Eq. 10. From this one can calculate the tissue D:

$$D = \frac{1}{A_d\Sigma(w_i/l_i)} \cdot \frac{1}{dt/(V dC'_R) - 2(1/P + \Delta x/D^0)/A_T}. \quad (14)$$

The critical question is the magnitude of the negative term in the denominator, the summed resistance of endothelial and unstirred layers. Ginzburg and Katchalsky (1963) showed that even with very ineffective stirring the unstirred layer was apparently only about 0.01 cm thick. When neglecting the endothelial barriers, the ratio, r, of the resistance of the two unstirred layers to the total resistance is approximately:

$$r = \frac{2\Delta x/(D^0A_T)}{\bar{l}/(DA_d) + 2\Delta x/(D^0A_T)} \doteq \frac{2\Delta x}{\bar{l}}\frac{D}{D^0}\frac{A_d}{A_T}. \quad (15)$$

For calcium, with a value of D/D^0 of about 0.25 and A_d/A_T of 0.4 (see Results) and, for a tissue slab 0.15 cm thick, the ratio is: $r < [2(0.01)/0.15](0.25)(0.4) < 0.013$. Thus, neglecting unstirred layer effects should not cause underestimation of D by more than 1%.

The permeability of the endothelial monolayers is not known. Use in Eq. 14 of values for P taken from estimates of the permeability of myocardial capillary endothelium, which is morphologically similar, suggested questionably high values of D, about $\frac{1}{2}$ of the free diffusion coefficient. To avoid dependence on such a quantitatively important assumption, the problem was attacked directly by performing a set of experiments from which D was determined after peeling off both endothelial layers. Although peeling must cause some damage, this was not very evident on examination with a dissection microscope or on histologic sections, since it apparently caused little or no tearing or separation of myocardial cells. The results show no significant differences in D's estimated with Eq. 10 from data obtained with and without endothelial layers (see Results). Therefore, in the subsequent analysis, the resistance of both endothelial and unstirred layers was neglected, that is, we used Eqs. 3–6 for sucrose and Eqs. 10–12 for calcium.

Partitioning of Solute between Bathing Medium and Diffusion Space

Partitioning of solute between the bathing medium and the diffusion space in the tissue will change either the driving force or the area available for diffusion. Thus in the steady state flux equation,

$$V dC^*_R/dt = -DA_wK_dC^*_D/\bar{l}, \quad (16)$$

K_d is a partition coefficient, and $K_dC^*_D$ is the tracer concentration at the donor side in the space available for water in the diffusion pathway, A_w. K_d would be greater than 1 in the unlikely case that the solute were more soluble in the water of the diffusion pathway than in the external medium. (If the solute were lipid-soluble and its diffusion not restricted to aqueous pathways, then D, A, and K_d should all be interpreted in another way and the analytical approaches presented here would have to be modified substantially.) For hydrophilic solutes, K_d will be less than 1.0 because of molecular exclusion of the solute from water in the con-

TABLE I

MOLECULAR SIZE AND PARTITION COEFFICIENTS K_d, IN MYOCARDIAL EXTRACELLULAR FLUID

Substance	Molecular radius	K_d
	Å	ml/ml
H_2O	1.3	1.00
Ca^{2+}	2.8	0.99*
Sucrose	5.5	0.975
Inulin	15	0.86

*Value obtained by interpolation from the other values.

nective tissue matrix of the interstitium. These are circumstances appropriate to our analysis; thus A_d is seen to be:

$$A_d = K_d A_w. \tag{17}$$

The data of Schafer and Johnson (1964) on rabbit hearts suggest values of K_d for sucrose and inulin of 0.975 and 0.86, defining K_d as 1.0 for water. Therefore, if we assume that the partitioning of solute between the bathing medium and ECF is a function only of hydrated molecular or ionic radius (i.e., steric exclusion of solute by the ground substance), K_d for calcium may be estimated to be 0.99 by linear interpolation, as in Table I. Partitioning of solute between the bathing media and the diffusion space may be neglected safely, at least for a sucrose-calcium comparison.

RESULTS

Typical curves for $C_R(t)$ are shown for sucrose and for calcium in Fig. 2. The appropriate equations have been fitted to the data, Eq. 3 for sucrose and Eq. 10 for calcium.

In the steady state linear portion of the curves, the slope of the calcium curve, $(dC_R/dt)_{Ca}$, was steeper than that of the corresponding sucrose curve, as might be expected from the free diffusion coefficients; these curves were typical, but there was a great deal of scatter. The time lags, T_s and T_{Ca}, increased with specimen thickness but varied only randomly with Ca_0 and with the osmolarity of the bathing solution.

Diffusion Coefficients

The free diffusion coefficient at 23°C for sucrose in water is 5.20×10^{-6} cm^2/s (Irani and Adamson, 1958) and for calcium is 7.78×10^{-6}cm^2/s (Wang, 1953); the ratio D^0_{Ca}/D^0_s is 1.53.

The apparent diffusion coefficient for sucrose, D_s in Eq. 3, was uninfluenced by changes in Ca_0 or external osmolarity over the range from 230 to 510 mosmol. D_s is plotted versus Ca_0 in Fig. 3, upper panel; the scatter, indicated by bars for ±1 SD, is great. From all the data, the mean D_s is $1.11 \pm 0.06 \times 10^{-6}$cm^2/s ($n$ = 74) (mean ± SEM). Thus D_s/D^0_s averaged 22%.

The average tortuosity coefficient, calculated from the average of the individual λ's

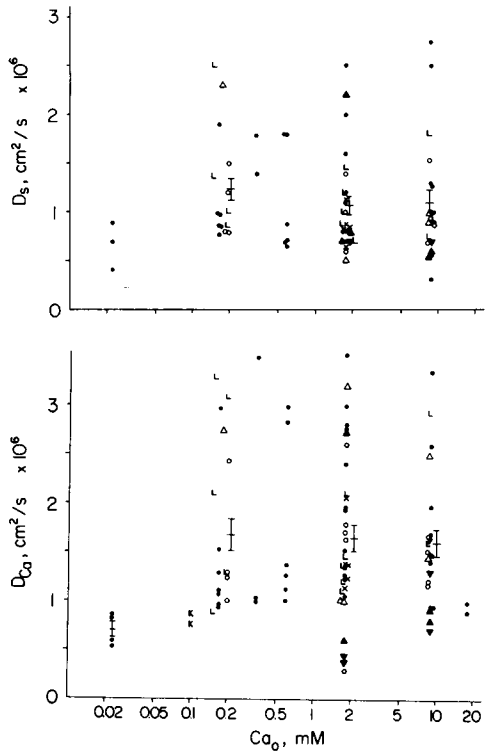

FIGURE 3 Diffusion coefficients for sucrose (upper panel) and calcium (lower panel) in myocardium, plotted as a function of external Ca^{2+} concentration. The vertical bars show ± 1 SEM around the means, the thin horizontal bars. The groupings in this and subsequent figures are at Ca_0 = 0.023, 0.1–0.6, 1.7–1.9, 8.5–9.0, and at 18.1 mM. Changes in Ca_0 and in osmolarity of the bathing medium (raised osmolarities, △ and ▲, reduced osmolarity, ▼) had no apparent effect, nor did changing Na^+ concentration (low Na_0, ○ and ▼, high Na_0, ▲). All others were at normal osmolarity and Na_0 but with varied Ca_0: ● = normal Tyrode, L = lanthanum chloride 0.1 mM, K = potassium concentration reduced to 0.6 mM, X = endothelial layers peeled off both surfaces.

obtained in each experiment from Eq. 2, where $\lambda_s^2 = D_s^0/D_s$, was 2.34 ± 0.06 (n = 74). This is similar to the value of 2.11 ± 0.035 (n = 10) found by Suenson et al. (1974) for sucrose in the same type of experiment. (Note that by using the mean D_s, the value of $\lambda = (D_s^0/D_s)^{1/2} = (5.1/1.114)^{1/2} = 2.14$, is not greatly different.)

The apparent diffusion coefficient for calcium, D_{Ca} in Eq. 11, is plotted versus Ca_0 in Fig. 3, lower panel. The mean D_{Ca} is 1.65 ± 0.10 × 10^{-6}cm²/s (n = 74); D_{Ca}/D_{Ca}^0 is 21%, The tortuosity coefficients, λ_{Ca}, averaged 2.40 ± 0.08 (n = 74), while D_{Ca}^0/ mean $D_{Ca})^{1/2}$ = 2.17. The data are not strongly suggestive of any influence of Ca_0 on D_{Ca}, but the paucity of data at the extremes of the range, at Ca_0 = 0.023 mM and 18 mM, leaves minor doubts. We report these extremes but hesitate to put much reliance on them: At Ca_0 = 18 mM there is real difficulty in maintaining the Ca in solution; at Ca_0 = 0.023 mM the question is whether or not the transient is completed.

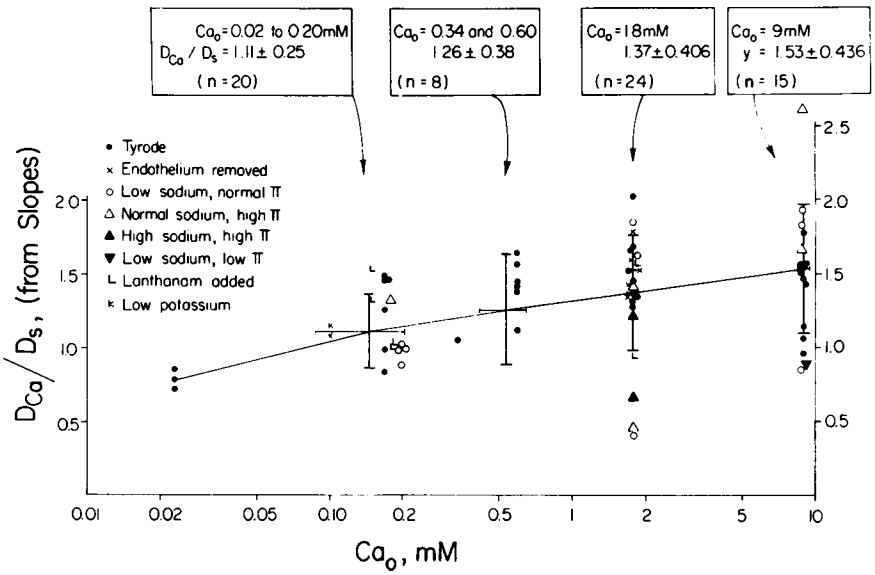

FIGURE 4 Ratio of apparent diffusion coefficient for calcium, D_{Ca}, to that for sucrose, D_s, calculated from the steady state slopes by Eq. 18: $D_{Ca}D_s \simeq [dC_R(t)]_{Ca}/[dC_R(t)]_s$. There appears to be a tendency for the ratio to be low at low Ca_0, perhaps because the transient is incomplete even with 6–8-h experiments; this would be compatible with the higher ratios of V_{dep}/V_d at low Ca_0, as can be expected with first-order binding (Eq. 35). At high Ca_0 the ratio approaches the ratio of free diffusion coefficients, 1.53.

(Stabilization of Ca_0 at low levels with Ca-EDTA buffer is not useful since we would then be measuring the combined rates of diffusion of Ca-EDTA and Ca.)

The ratio D_{Ca}/D_s is of particular value because of one's confidence in sucrose as an inert extracellular marker. Eqs. 10 and 12 provide the slopes of dC_R/dt in the steady state; the ratios of the slopes is given by dividing the first terms of the two equations:

$$(dC_R/dt)_{Ca}/(dC_R/dt)_s = D_{Ca}A_{dCa}/D_sA_{ds} \simeq D_{Ca}/D_s. \quad (18)$$

This calculation avoids errors due to using the intercepts T_{Ca} and T_s or the estimates of A_d or the distribution of thicknesses, l_i, necessarily inherent to the calculation of D by Eqs. 4 or 11. The ratio of final slopes is plotted in Fig. 4. The data are grouped for the purpose of calculating mean estimates of D_{Ca}/D_s at various Ca_0; the error bars are ± 1 SD (not S.E.M). There is an apparent tendency for higher ratios at higher Ca_0; the mean ratio for all the simultaneous paired slopes was 1.32 ± 0.05 (n = 67), but for Ca_0 = 1.8 and 9 mM was 1.43 ± 0.07 (n = 39) (means ± SEM).

The question raised by these estimates is whether it is possible that $(dC_R/dt)_{Ca}$ might not have reached its final steady state values at low Ca_0, even though the experiments lasted 6–9 h, and showed abscissal intercepts, $T_{Ca}/\bar{l}$, of 200–1,300 min/cm (average = 676 ± 348 min/cm) (n = 92). Data concerning V_{dep} (below) support this idea, which only points out that failure to observe a subtle curvature in $C(t)$ can result in underestimation of D_{Ca}/D_s from the radio of slopes at low Ca_0. The explana-

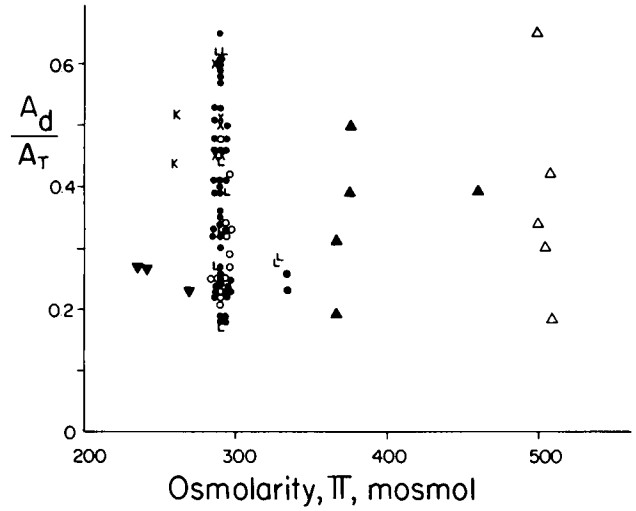

FIGURE 5 Apparent fractional area for the diffusion path, A_d/A_T (cm^2/cm^2 sheet), or V_d/V_T(ml/ml), plotted versus the osmolarity of the bathing medium, π_0, (mosmol). No trend was apparent. A_d/A_T averaged 0.41 ± 0.15 (SD) (n = 74).

tion is not likely to lie in the ratio A_{dCa}/A_{ds} being greatly different from unity; Table I would suggest perhaps a 1.5% difference and we see no reason to imagine the difference to be much larger.

The diffusion coefficients were not obviously influenced by raising the osmolarity with sucrose or sodium, or replacing Na^+ with sucrose, all of which raise the viscosity of the solution. The data are shown in Fig. 3, where the symbols are the same as in Figs. 4 and 5. Nor were the D's any higher when the osmolarity was reduced (the ▼'s).

Area of the Diffusion Path, A_d

The A_d's were calculated for sucrose and calcium by Eq. 5. No systematic influences (statistically significant or suggestive) of external osmolarity or of Ca_0 could be seen in the data; for example, see A_d versus osmolarity in Fig. 5. This seems somewhat surprising since one would anticipate the myocardial cells to behave more or less as osmometers, to swell in hyposmolar solutions and to shrink in hyperosmolar media; at π = 500 mosmol, one would guess the cells to be about 300/500 of their original size, in accordance with the observations of Blinks (1965) and of Birks and Davey (1969) and that the paucity of sarcoplasmic reticulum in cardiac muscle would not permit its swelling to offset any shrinkage. We did not measure cell diameters in the frozen sections. The probable explanation is that the cells do shrink at high π but the interstitium retains its shape and volume, there being no mechanism for maintaining total tissue volume or any force for expanding the interstitium.

The values of A_d/A_T or V_d/V_T were 0.41 ± 0.15 (SD; n = 74). Statistically, this mean value is higher than the value of 0.22 ± 0.07 (n = 10) found by Suenson et al. (1974) in our laboratory, using the same techniques; however we feel that our earlier

value is quite compatible with the present observations shown in the group at 290 mosmol in Fig. 5. A_d should include all extracellular space; our mean value is similar to the estimates of sucrose space found by Schafer and Johnson (1964) in rabbit heart, which is reasonable since ours were soaked in oxygenated Tyrode solution for several hours and theirs were rabbit hearts perfused with Tyrode. Our preparation does contain more water than normal, and A_d/A_T is higher than in vivo estimates of ECF space: Polimeni (1974) estimated the extracellular space to be 0.19 ml/ml tissue in normal in vivo rat hearts using $^{32}SO_4$ space and stereologic measurements. This abnormality of the preparation might result in our estimates of D_s and D_{Ca} being higher than normal in vivo values; in a preparation with less expansion of the ECF the tortuosity coefficients might actually be higher, and it is also possible that the ratio A_{dCa}/A_{ds} might be larger than 1.015 because of increased importance of exclusion effects. Interstitial expansion can be expected to influence A_d's and D's for large molecules such as albumin (Wiederhielm et al., 1976), but will have little effect on small molecules.

Dead-End Pore Volume for Calcium, V_{dep}:

The dead-end pore volume for Ca is a virtual volume in which there is a Ca concentration in equilibrium with that on the diffusion channel. The physical interpretation of V_{dep} is simple and should not be lost from sight in a maze of formulations. It is the volume which contains all the calcium with which tracer has equilibrated, minus that in the diffusion space. This is simply a statement of conservation of mass. The diffusion space is taken to be the same as that for sucrose, V_d, so that V_{dep}/V_d is:

$$\frac{V_{dep}}{V_d} = \frac{\text{steady state volume of distribution of calcium}}{\text{steady state volume of distribution of sucrose}} - 1. \quad (19)$$

A difference in molecular diffusion coefficient must be taken into account in the translation from the intercepts. Eqs. 20–24*b* do this explicitly. The translation of Eq. 19 that we feel is least subject to experimental and analytical error is Eq. 24*b*; in the next paragraphs we relate the development so that the reasons may be evident to the reader.

We emphasize that the dead-end pore model is a simplified approximation to reality since it represents only one first-order pool with a single exchange rate K_e. In steady state it should give a reasonably good estimate of the total pool size, V_{dep}; the estimation of K_e is quite inexact, and precludes meaningful expansion of the analysis in terms of the several different K_e's for the different sites of sequestration. In these experiments we look for changes in the pool size for Ca^{2+} at different calcium concentrations. Since the calculation of the sum of V_{dep} plus V_d is based on mass conservation and does not depend at all on K_e, the estimation of V_{dep} is almost independent of the form of the model and should provide a fairly good estimate of the pool size in any established steady state.

The intercepts or time lags should define the amount of tracer in the specimen at steady state. The abscissal intercept, T_{Ca}, provides a basis for the estimation of

V_{dep} by comparison with the intercept or time lag for sucrose. At time $t = T_s$ the sum of the first two terms of Eq. 3 is zero; T_{Ca} is obtained similarly from Eq. 10. Taking ratios of the first terms and second terms, we obtain:

$$\frac{\frac{D_{Ca}A_{dCa}T_{Ca}}{V}\sum\frac{w_i}{l_i}}{\frac{D_sA_{ds}T_s}{V}\sum\frac{w_i}{l_i}} = \frac{\frac{\bar{l}A_{dCa} + V_{dep}}{6V}}{\frac{\bar{l}A_{ds}}{6V}}, \tag{20a}$$

or

$$D_{Ca}T_{Ca}/D_sT_s = 1 + V_{depCa}/V_{dCa} = 1 + V_{dep}/V_d. \tag{20b}$$

No assumptions concerning A_d's have been made in Eq. 20*b*, which holds even if $A_{ds} \neq A_{dCa}$, or if $V_{ds} \neq V_{dCa}$. To obtain V_{dep}/V_d without going through the model analysis, thereby keeping as close to the experimental data as possible, one of two reasonable assumptions may be made: one would assume Eq. 18 to be correct and substitute $(dC_R/dt)_{Ca}/(dC_R/dt)_s$ for D_{Ca}/D_s; the other would assume $D_{Ca}/D_s = D^0_{Ca}/D^0_s = 1.53$. We prefer the latter assumption, giving us:

$$V_{dep}/V_d = D^0_{Ca}T_{Ca}/D^0_sT_s - 1 = 1.53\ T_{Ca}/T_s - 1 \tag{21}$$

Implicit in the use of 1.53 instead of the ratio of slopes is the thought that the final slopes for Ca may not yet represent the steady state, i.e. may err on the low side. This is likelier at low Ca_0, as suggested by Fig. 4, than at normal or high concentrations. If the slope is too low, then T_{Ca} will also be too small, and V_{dep} will therefore be underestimated by Eq. 21, particularly at low Ca_0 (assuming T_s to be unaffected); a partial correction is provided by using 1.53 instead of the observed ratio of slopes.

An improved estimate of V_{dep}/V_d, at least partially corrected for incompleteness of the transient, can be obtained by applying the idea that $(dC_R/dt)_s$ will have reached the steady state (since there is no dead-end pore for sucrose) and that one can predict the calcium steady state slope from it, following the idea of Eq. 9: $(dC_R/dt)_{Ca}$ in steady state $= A_{dCa}D^0_{Ca}/A_{ds}D^0_s \cdot (dC_R/dt)_s$ at final slope. Assuming then that only the last experimental point, $C_R(t_{end})_{Ca}$, of $C_r(t)$ for calcium represents the steady state, and that $A_{dCa} = A_{ds}$, then a new value of the intercept, T'_{Ca}, may be calculated by simple triangulation from the point and the slope:

$$T'_{Ca} = t_{end} - C_R(t_{end})_{Ca}/[1.53 \times \text{final slope } (dC_R/dt)_s] \tag{22}$$

T'_{Ca} will be systematically greater than T_{Ca} whenever the transient for Ca is incomplete and non-steady state points are used in calculating the slope. With T'_{Ca}, the estimate of V_{dep}/V_d is:

$$V_{dep}/V_d = (D^0_{Ca}/D^0_s)(T'_{Ca}/T_s) - 1 = 1.53\ T'_{Ca}/T_s - 1 \tag{23}$$

A minor modification to reduce the error due to variation in a single sample can be made by substituting for the final slope $(dC_R/dt)_s$ so as to use the estimate of $C_R(t_{end})_s$

for the same sample as for Ca and canceling out any sampling volume error. The substitution is to use Eq. 22 for T'_{Ca} and $(dC_R/dt)_s = C_R(t_{end})_s/(t_{end} - T_s)$ giving a slightly more complex calculation, but one rather directly made from the raw data:

$$\frac{V_{dep}}{V_d} = \frac{D^0_{Ca}}{D^0_s}\frac{t_{end}}{T_s} - \frac{(t_{end} - T_s)}{T_s}\cdot\frac{C_R(t_{end})_{Ca}}{C_R(t_{end})_s} - 1, \qquad (24a)$$

or

$$\frac{V_{dep}}{V_d} = \frac{1}{T_s}\left[1.53\, t_{end} - (t_{end} - T_s)\frac{C_R(t_{end})_{Ca}}{C_R(t_{end})_s} - T_s\right] \qquad (24b)$$

Eq. 24 gives an estimate of V_{dep}/V_d partially or completely corrected for a prolonged Ca transient. (It cannot give a systematic overcorrection.) Eq. 21 allows estimation of V_{dep}/V_d from the observed intercepts without correction. Eq. 12 provides an estimate from the modeling; although it is conceptually similar to Eq. 21 it contains errors due to the accumulation of the errors in the estimates of D_{Ca}, T_{Ca}, A_d, $\bar{l}$, and $\sum(w_i/l_i)$. The three estimates are shown in Fig. 6. The values of V_{dep}/V_d from Eq. 12 (left panel) exhibit a great deal of scatter and no trend can be observed. Eq. 21 (middle panel) gives values with substantially less scatter, as expected. Eq. 24 (right panel) provides no further decrease in scatter, but the values are somewhat higher than

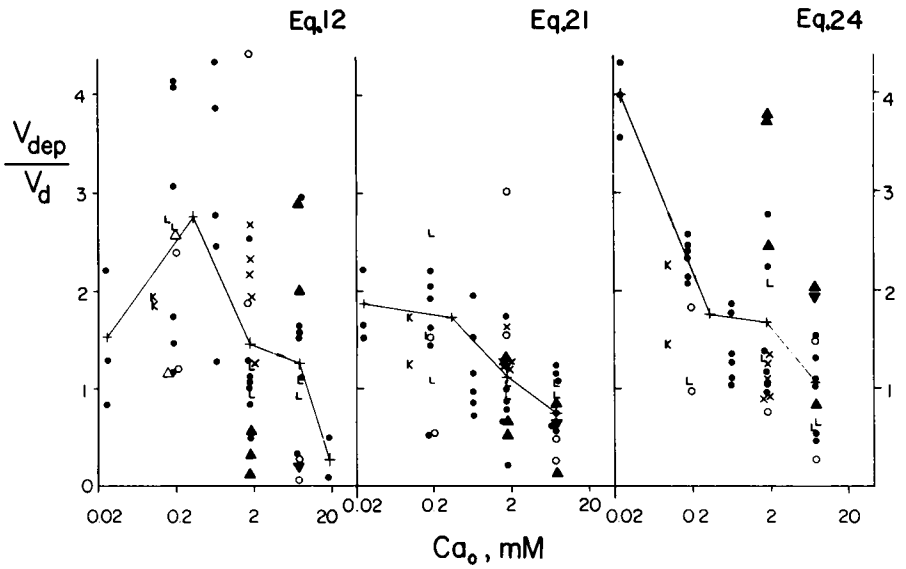

FIGURE 6 V_{dep}/V_d, the volume of distribution of Ca^{2+} outside of the diffusion channel to that inside, as a function of Ca_0. Three different calculations are shown: from model fitting by Eq. 12 (left panel); from the abscissal intercepts of $C_R(t)$, the time lags, by Eq. 21 (middle panel); and from the final values of $C_R(t)$ and the intercepts by Eq. 24 (right panel). The scattering of values given by the multiparameter modeling (left panel) is reduced by making the calculation more directly from the data (middle and right panels). V_{dep}/V_d is not dramatically affected by Ca_0 but appears to be higher at low Ca_0.

for Eq. 21. We feel that Eq. 24 is more likely to give correct values, adhering to the principle that the best estimates are those calculated most directly from the data without intermediate calculation and assumptions.

Apparent Diffusion Coefficients for Ca during a Diffusional Transient

In this section we introduce derivations for two apparent diffusion coefficients, D'_{Ca} and D''_{Ca}, neither of which is the effective diffusion coefficient D_{Ca} estimated from our steady state data. Both are important because they can be used to estimate the rate of progress of a diffusional front, both apply to transient states. We define D'_{Ca} as the apparent diffusion coefficient for tracer calcium when Ca_0 is constant; D''_{Ca} is that for a change in Ca_0 in the tissue after a step change at the surface.

Following the proposal of Bassingthwaighte and Reuter (1972), we will derive Eq. 2 using a one-dimensional diffusion equation, where the rate of change of concentration at a point is influenced by first-order binding to an immobile substance B, forming a complex CaB:

$$\frac{\partial Ca}{\partial t} + \frac{\partial CaB}{\partial t} = D_{Ca}(\partial^2 Ca/\partial x^2), \tag{25}$$

where Ca is the concentration of free calcium, CaB is the concentration of calcium on a binding site, and x is distance. But for first-order binding, CaB is given by the mass law relationship for the equilibrium:

$$Ca \cdot B/CaB = K_b, \tag{26}$$

where B is the concentration of uncomplexed binding sites and K_b is an apparent first-order binding constant. The total binding-site concentration B_T is constant, and

$$CaB + B = B_T. \tag{27}$$

The partial derivative $\partial CaB/\partial t$ can be derived from Eq. 26 by the chain rule, which gives:

$$\frac{\partial CaB}{\partial t} = \frac{\partial CaB}{\partial Ca} \cdot \frac{\partial Ca}{\partial t} = \frac{\partial Ca}{\partial t} \cdot \frac{K_b B_T}{(K_b + Ca)^2}. \tag{28}$$

Substituting in Eq. 25 and cross-multiplying gives

$$\frac{\partial Ca}{\partial t} = \frac{D_{Ca}}{1 + K_b B_T/(K_b + Ca)^2} \frac{\partial^2 Ca}{\partial x^2} = D''_{Ca} \frac{\partial^2 Ca}{\partial x^2}, \tag{29}$$

which defines the apparent diffusion coefficient D''_{Ca} for nontracer calcium during a concentration change:

$$D''_{Ca} = D_{Ca}/[1 + K_b B_T/(K_b + Ca)^2]. \tag{30}$$

Similarly, in the presence of a family of independent immobile binding sites with individual total concentrations, B_{Ti}, binding constants K_{bi}, and N_b members:

$$(\partial Ca/\partial t)\left(1 + \sum_{i=1}^{N_b} [K_{bi}B_{Ti}/(K_{bi} + Ca)^2]\right) = D_{Ca}(\partial^2 Ca/\partial x^2) \tag{31}$$

so that D''_{Ca} is

$$D''_{Ca} = \frac{D_{Ca}}{1 + \sum_{i=1}^{N_b} K_{bi}B_{Ti}/(K_{bi} + Ca)^2}. \tag{32}$$

This equation should *not* be compared to Eq. 2 to suggest an interpretation for V_{dep} in terms of one or more binding sites, because Eq. 32 is valid only when Ca concentration and V_{dep} are changing; thus,

$$1 + \frac{V_{dep}}{V_d} \neq 1 + \sum_{i=1}^{i=N_b} K_{bi}B_{Ti}/(K_{bi} + Ca)^2. \tag{33}$$

This point is brought out to emphasize the difference between tracer fluxes and net fluxes of mother substance.

The diffusion of tracer is a simpler process because at any given constant concentration of nontracer Ca, the volume of distribution, $V_d + V_{dep}$, is fixed, and there is no retardation of the tracer diffusion front by changes in the local concentrations. Thus in Eq. 25 the ratio of tracer ^{45}Ca to tracer ^{45}CaB is a constant. From Eq. 26,

$$\frac{V_{dep}}{V_d} = \frac{^{45}CaB}{^{45}Ca} = \frac{CaB}{Ca} = \frac{B}{K_b}, \tag{34}$$

and using Eq. 27, considering Ca constant,

$$\frac{^{45}CaB}{^{45}Ca} = \frac{B_T}{Ca + K_b} = \frac{V_{dep}}{V_d}. \tag{35}$$

Substituting for CaB in Eq. 26 gives

$$\frac{\partial\, ^{45}Ca}{\partial t}\left(1 + \frac{B_T}{Ca + K_b}\right) = D_{Ca}\frac{\partial^2(^{45}Ca)}{\partial x^2}. \tag{36}$$

This defines the apparent diffusion coefficient for tracer at steady Ca_0 as D'_{Ca}:

$$D'_{Ca} = \frac{D_{Ca}}{1 + B_T/(Ca + K_b)},$$

$$= \frac{D_{Ca}}{1 + V_{dep}/V_d} = D_{Ca}\cdot\frac{V_d}{V_d + V_{dep}}. \tag{37}$$

The latter forms follow from Eq. 34. Now Eq. 37 is identical to Eq. 2 and puts it on a mathematical basis rather than an intuitive one. (Now it is relevant to point out that Niedergerke [1957] should have used D''_{Ca}, Eq. 30, rather than D'_{Ca}, Eq. 37, since he was

changing Ca_0; actually, in his experiments the difference was slight, since the changes in Ca_0 were small, going from 1 to 2 mM.)

Calcium Binding and V_{dep}

Eq. 34 defined V_{dep} in terms of binding to a single site, a dependency quantitatively different from a passively exchanging fluid volume. When several independent first-order binding sites are present, then

$$\frac{V_{dep}}{V_d} = \frac{1}{Ca} \sum_{i=1}^{N_b} CaB_i = \sum_{i=1}^{i=N_b} B_{Ti}/(Ca + K_{bi}), \tag{38}$$

which defines a model for the concentration-dependency of V_{dep} in terms of multiple binding sites. To fit the observed V_{dep}/V_d with Eq. 38 has something of the style of multi-exponential analysis; that is, it is an oversimplification to consider only the sum of first-order processes, but there is nevertheless some merit in determining the minimum number of binding processes required to explain the data.

In the upper panel of Fig. 7 is plotted a nondimensionalized version of V_{dep}/V_d

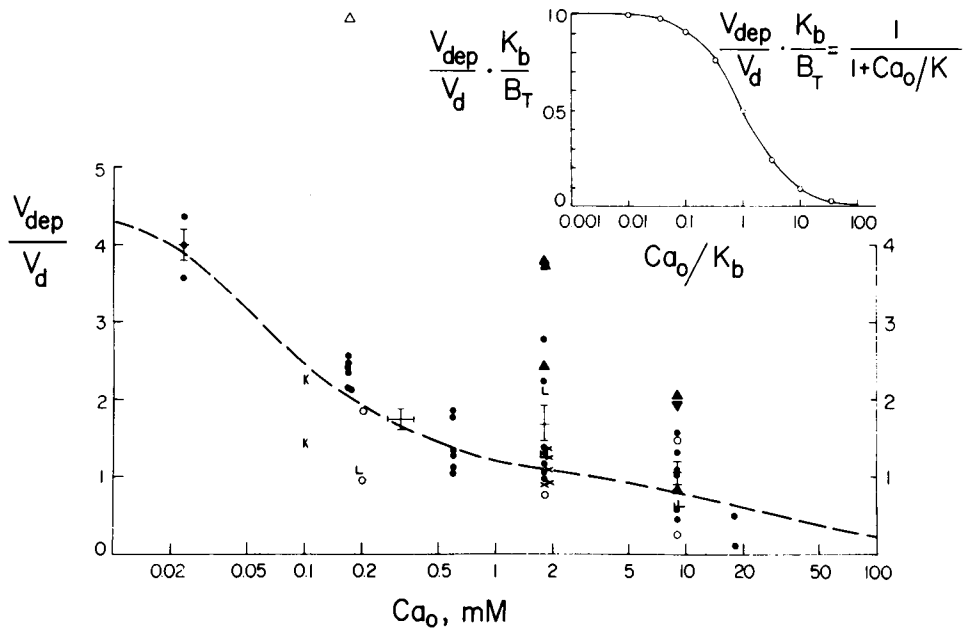

FIGURE 7 A sum of first-order binding processes as a descriptor of V_{dep}/V_d at varied Ca_0. *Insert panel:* The curve for equilibrium binding, Eq. 35, is given in nondimensional form. Raising Ca_0 reduces the ratio of bound to free Ca, although the absolute volumes of distribution, V_{dep} and V_d, are both increased. *Figure:* Values of V_{dep}/V_d were calculated by Eq. 24; the means and SD are given for the same concentration regions as were used in Figs. 3, 4, and 6. The theoretical curve is for two hypothetical binding sites, one a site with a fairly high affinity for Ca ($K_b = 6 \times 10^{-5}$ M) but in low concentration ($B_T = 24 \times 10^{-5}$ M) and the other a low affinity site with a high concentration ($K_b = 0.03$ M, $B_T = 0.03$ M).

taken from Eq. 35. In the lower panel the data for V_{dep}/V_d by Eq. 24 are fitted by using Eq. 38 and assuming only two binding sites. A single binding site equation cannot be reasonably fitted to the data. In view of the large scatter in the data, the particular values given for the K_b's and B_T's cannot be considered accurate, but it seems reasonable to conclude that at least two sites are available: one high affinity and low concentration, and the other with low affinity and relatively high concentration.

Studies by Catchpole and co-workers indicate that the fixed negative charge density of these substances range from 35 meq/kg tissue water for loose connective tissues (tendon) to 160 meq/kg tissue for dense connective tissues (cartilage) (Joseph et al., 1959); the former figure might be a reasonable estimate of B_T for the ground substance in the ECS of muscle. In addition, the equilibrium constant for binding of calcium to the substance, $Ca^{2+} \cdot B^{2-}/CaB$, is about 26 mM for a wide range of tissues (Engel et al., 1954). Thus the identification of the low affinity binding site with interstitial connective tissue components appears reasonable.

The Influence of Competing Cations on V_{dep}

If the number of available binding sites for Ca is influenced by changes in Na_0, this will result in a change in V_{dep}. The possibilities include direct competition by other alkali metal cations or by hydrogen ion, allosteric influences, noncompetitive blocking of sites, etc. Lacking more specific insight, let us examine a likely and relatively straightforward possibility, combination of the binding site with one or two Na^+ instead of one Ca^{2+}. With the same nomenclature as in Eqs. 27 and 28, B_T is the sum of the concentrations:

$$CaB + NaB + Na_2B + B = B_T, \tag{39}$$

and

$$\frac{Na \cdot B}{NaB} = K_{Na}; \quad \frac{Na^2 \cdot B}{Na_2B} = K_{2Na}. \tag{40}$$

Substitution into Eq. 39 gives:

$$B\left(1 + \frac{Ca}{K_b} + \frac{Na}{K_{Na}} + \frac{Na^2}{K_{2Na}}\right) = B_T \tag{41}$$

From Eq. 27, $CaB/Ca = B/K_b$, so the dead-end pore volume for Ca becomes

$$\frac{V_{dep}}{V_d} = \frac{CaB}{Ca} = \frac{B}{K_b} = \frac{B_T}{K_b\left(1 + \frac{Ca}{K_b} + \frac{Na}{K_{Na}} + \frac{Na^2}{K_{2Na}}\right)} \tag{42}$$

This is analogous to Eq. 35, to which it reduces when $Na_0 = 0$.

Affinity of the Ca binding site for sodium would result in a competition between Na and Ca for the site. Raising Na_0 in this circumstance would be expected to reduce V_{dep}/V_d and the reduction would be greater if the affinity for Na were higher. How-

ever, the data of Fig. 6 do not exhibit such a trend. If anything, the opposite might be occurring; there is a suggestion that lowering Na_0 decreased V_{dep}/V_d. Joseph et al. (1954) have observed Na to be a weaker competitor for Ca binding sites in a connective tissue matrix; our failure to show a distinct sodium effect may be attributable simply to the same low affinity. On the other hand, Joseph et al. observed that the effect of potassium was greater than for sodium. Our two experiments at K_0 = 0.6 mM and Ca_0 = 0.1 mM showed no increase in V_{dep}/V_d and suggest that there were few or no binding sites with potassium binding constants between 0.6 and 5.4 mM K^+. Experiments at high K_0 would be required in an exploration for sites with low potassium affinity.

CONCLUSIONS

Tortuosity coefficients, λ, for diffusion through the ECS of heart muscle are slightly over 2.0, so that the effective diffusion coefficients D for hydrophilic substances that do not diffuse through muscle cells were about $1/\lambda^2$ or 22% of the free diffusion coefficient in water.

In the steady state, where there are no changes in concentrations, the rates of diffusion are not influenced by the presence of binding sites or of sequestered spaces for the diffusing molecules. This is simply because the fraction of tracer molecules sequestered is not changing.

In a transient state, for tracer or for nontracer chemical concentrations, the presence of binding sites prolongs the transient. The prolongation is at least proportional to the ratio of total apparent volume of distribution (binding sites or sequestered space, V_{dep}, plus diffusion space, V_d) to the volume of the diffusion space, V_d. The prolongation is greater if the rate of equilibration (K_e) between solute in the diffusion space and that in the sequestered space is slow.

Data on the cat myocardium suggest that at least two binding sites for calcium are accessible. One is a moderately high affinity site in low concentration, and the other is a high concentration, low affinity site, probably a component of the connective tissue.

The authors wish to acknowledge the expert technical assistance of Allan R. Wanek and of E. Anne Bassingthwaighte in the performance of these experiments and in their analysis. Sylvia Danielson has prepared the manuscript and Hedi Nurk the illustrations.

This work was supported by grants from the National Institutes of Health (HL 19139 and HL 19135), the American Heart Association (74-1025), and the Minnesota Heart Association.

Received for publication 9 March 1977 and in revised form 20 June 1977.

APPENDIX I

The Tortuosity Factor, λ

The thickness of the sheet in Fig. 1 is l, which would be the diffusion distance if the medium were a free fluid. We define λ as the ratio of the length of the tortuous pathway of local

cross-sectional area A_d to l. If the volume of the pathways in the sheet through which diffusion can occur is V_P, then

$$A_d = V_P/l, \tag{43}$$

but the effective length of the pathway is λl so that the apparent diffusional area, for the same volume V_P, is A_P:

$$A_P = A_d/\lambda = V_P/\lambda l. \tag{44}$$

By writing the steady-state Fick diffusion equation, the flux J across the sheet along all of the tortuous path in parallel:

$$J = D^0 A_P(\Delta c/\lambda l), \tag{45}$$

and substituting for A_P from Eq. 44 gives

$$J = (D^0/\lambda^2) A_d(\Delta c/l). \tag{46}$$

Thus λ^2, rather than λ, is used in Eq. 1 and subsequent equations.

REFERENCES

ALDRICH, B. I. 1958. The effects of the hyaluronic acid complex on the distribution of ions. *Biochem. J.* **70**:236–244.

BARRER, R. M. 1953. A new approach to gas flow in capillary systems. *J. Phys. Chem.* **57**:35–40.

BASSINGTHWAIGHTE, J. B., and H. REUTER. 1972. Calcium movements and excitation-contraction coupling in cardiac cells. *In* Electrical Phenomena in the Heart. W. C. DeMello, editor. Academic Press, Inc. New York, 353–395.

BEELER, G. W., JR., and H. REUTER. 1970. Membrane calcium current in ventricular myocardial fibres. *J. Physiol. (Lond.).* **207**:191–209.

BIRKS, R. I., and D. F. DAVEY. 1969. Osmotic responses demonstrating the extracellular character of the sarcoplasmic reticulum. *J. Physiol. (Lond.).* **202**:171–188.

BLINKS, J. R. 1965. Influence of osmotic strength on cross-section and volume of isolated single muscle fibres. *J. Physiol. (Lond.).* **177**:42–57.

CAILLÉ, J. P., and J. A. M. HINKE. 1972. Evidence for Na sequestration in muscle from Na diffusion measurements. *Can. J. Physiol. Pharmacol.* **50**:228–237.

CRANK, J. 1956. The Mathematics of Diffusion. The Oxford University Press, London, U.K. 347.

ENGEL, M. B., N. R. JOSEPH, and H. R. CATCHPOLE. 1954. Homeostasis of connective tissues. I. Calcium-sodium equilibrium. *Arch. Pathol.* **58**:26–39.

ENGEL, M. B., N. R. JOSEPH, D. M. LASKIN, and H. R. CATCHPOLE. 1961. Binding of anions by connective tissue: dermis and cartilage. *Am. J. Physiol.* **201**:621–627.

FAWCETT, D. W., and N. S. MCNUTT. 1969. The ultrastructure of the cat myocardium. I. Ventricular papillary muscle. *J. Cell. Biol.* **42**:1–45.

GERSH, I., and H. R. CATCHPOLE. 1960. The nature of ground substance of connective tissue. *Perspect. Biol. Med.* **3**:282–319.

GINZBURG, B. Z., and A. KATCHALSKY. 1963. The frictional coefficients of the flows of nonelectrolytes through artificial membranes. *J. Gen. Physiol.* **47**:403–418.

GOODKNIGHT, R. C., and I. FATT. 1961. The diffusion time-lag in porous media with dead-end pore volume. *J. Phys. Chem.* **65**:1709–1712.

HALJAMÄE, H., A. LINDE, and B. AMUNDSON. 1974. Comparative analyses of capsular fluid and interstitial fluid. *Am. J. Physiol.* **227**:1199–1205.

HODGKIN, A. L., and R. D. KEYNES. 1953. The mobility and diffusion coefficient of potassium in giant axons from *Sepia*. *J. Physiol. (Lond.).* **119**:513–528.

IRANI, R. R., and A. W. ADAMSON. 1958. Transport processes in binary liquid systems. I. Diffusion in the sucrose-water system at 25°. *J. Phys. Chem.* **62**:1517–1521.

JOHNSON, M. F. L., and W. E. STEWART. 1965. Pore structure and gaseous diffusion in solid catalysts. *J. Catal.* **4**:248–252.

JOSEPH, N. R., M. B. ENGEL, and H. R. CATCHPOLE. 1954. Homeostasis of connective tissues. II. Potassium-sodium equilibrium. *Arch. Pathol.* **58**:40–58.

JOSEPH, N. R., H. R. CATCHPOLE, D. M. LASKIN, and M. B. ENGEL. 1959. Titration curves of colloidal surfaces. II. Connective tissues. *Arch. Biochem. Biophys.* **84**:224–242.

KUSHMERICK, M. J., and R. J. PODOLSKY. 1969. Ionic mobility in muscle cells. *Science (Wash. D.C.)* **166**: 1297–1298.

LANGER, G. A., and J. S. FRANK. 1972. Lanthanum in heart cell culture: Effect on calcium exchange correlated with its localization. *J. Cell. Biol.* **54**:441–455.

LAURENT, T. C. 1970. The structure and function of the intercellular polysaccharides in connective tissue. *In* Capillary Permeability. C. Crone and N. A. Lassen, editors, Munksgaard, Copenhagen, Denmark. 261–277.

LONGSWORTH, L. G. 1953. Diffusion measurements, at 25°, of aqueous solutions of amino acids, peptides and sugars. *J. Am. Chem. Soc.* **75**:5705–5709.

MANERY, J. F. 1966. Connective tissue electrolytes. *Fed. Proc.* **25**:1799.

MARTINEZ-PALOMO, A., D. BENITEZ, and J. ALANIS. 1973. Selective deposition of lanthanum in mammalian cardiac cell membranes. *J. Cell. Biol.* **58**:1–10.

MORAD, M., and GOLDMAN, Y. 1973. Excitation-contraction coupling in heart muscle: membrane control of development of tension. *Prog. Biophys. Mol. Biol.* **27**:257–313.

NIEDERGERKE, R. 1957. The rate of action of calcium ions on the contraction of the heart. *J. Physiol. (Lond.).* **138**:506–515.

PAGE, E. 1963. Extracellular diffusion in cat heart muscle. *Biophys. Soc. Abstracts*, WC9.

PAGE, E., and R. S. BERNSTEIN. 1964. Cat heart muscle *in vitro*. V. Diffusion through a sheet of right ventricle. *J. Gen. Physiol.* **47**:1129–1140.

PATLAK, C. J., and J. D. FENSTERMACHER. 1975. Measurements of dog blood-brain transfer constants by ventriculocisternal perfusion. *Am. J. Physiol.* **229**:877–884.

PHILPOTT, G. W., and M. A. GOLDSTEIN. 1967. Sarcoplasmic reticulum of striated muscle: localization of potential calcium binding sites. *Science (Wash. D.C.).* **155**:1019–1021.

POLIMENI, P. 1974. Extracellular space and ionic distribution in cat ventricle. *Am. J. Physiol.* **227**:676–683.

REUTER, H., and N. SEITZ. 1968. Dependence of calcium efflux from cardiac muscle on temperature and external ion composition. *J. Physiol. (Lond.).* **195**:451–470.

SCHAFER, D. E., and J. A. JOHNSON. 1964. Permeability of mammalian heart capillaries to sucrose and inulin. *Am. J. Physiol.* **206**:985–991.

SHAW, M. 1976. Interpretation of osmotic pressure in solutions of one and two nondiffusible components. *Biophys. J.* **16**:43–57.

STOKES, R. H. 1950. An improved diaphragm-cell for diffusion studies, and some tests of the method. *J. Am. Chem. Soc.* **72**:763–767.

SUENSON, M., D. R. RICHMOND, and J. B. BASSINGTHWAIGHTE. 1974. Diffusion of sucrose, sodium and water in ventricular myocardium. *Am. J. Physiol.* **227**:1116–1123.

WANG, J. H. 1953. Tracer-diffusion in liquids. IV. Self-diffusion of calcium ion and chloride ion in aqueous calcium chloride solutions. *J. Am. Chem. Soc.* **75**:1769–1770.

WEIDMANN, S. 1966. The diffusion of radiopotassium across intercalated disks of mammalian cardiac muscle. *J. Physiol. (Lond.).* **187**:323–342.

WEINGART, R. 1974. The permeability to tetraethylammonium ions of the surface membrane and the intercalated disks of sheep and calf myocardium. *J. Physiol. (Lond.).* **240**:741–762.

WIEDERHIELM, C. A., J. R. FOX, and D. R. LEE. 1976. Ground substance mucopolysaccharides and plasma proteins: their role in capillary water balance. *Am. J. Physiol.* **230**:1121–1125.